ResearchGate

See discussions, stats, and author profiles for this publication at: https://www.researchgate.net/publication/231631747

Spontaneous Polarization Vector Reorientation Photorefractive Effect in Dye-Doped Ferroelectric Liquid Crystals

ARTICLE *in* THE JOURNAL OF PHYSICAL CHEMISTRY B · FEBRUARY 2002

Impact Factor: 3.3 · DOI: 10.1021/jp0134493

CITATIONS
23

READS
14

3 AUTHORS, INCLUDING:

Takeo Sasaki
Tokyo University of Science
78 PUBLICATIONS **975** CITATIONS

SEE PROFILE

Available from: Takeo Sasaki
Retrieved on: 25 January 2016

Spontaneous Polarization Vector Reorientation Photorefractive Effect in Dye-Doped Ferroelectric Liquid Crystals

Takeo Sasaki,* Atsushi Katsuragi, and Kazuo Ohno

Department of Chemistry, Faculty of Science, Science University of Tokyo, 1-3 Kagurazaka, Shinjuku-ku, Tokyo 162-8601, Japan

Received: September 10, 2001; In Final Form: December 20, 2001

The photorefractive effect of a series of low-molecular-weight ferroelectric liquid crystals (FLCs) doped with photoconductive compounds was investigated through two-beam coupling experiments. Asymmetric energy exchange was observed only in the ferroelectric phase, and the refractive index formation time was found to be ∼30 ms, which is faster than that of nematic photorefractive LCs. These results indicate that the mechanism of the photorefractive effect in FLCs differs from that in nematic LCs. The photorefractivity of a photoconductive polymer and FLC mixture was also investigated, and the effects of temperature, the strength of the applied electric field, and spontaneous polarization on the diffraction efficiency were examined.

Introduction

The photorefractive effect of organic materials has recently attracted great interest. The photorefractive effect is defined as the optical modulation of the refractive index of a medium as a result of a number of processes. The interference of two laser beams in a photorefractive material establishes a refractive index grating. The mechanism responsible for the formation of this refractive index grating is the generation of a space-charge field (internal electric field) due to charge separation between bright and dark areas of the interference and a subsequent change in the refractive index via an electrooptic effect (Pockels effect). A characteristic of the photorefractive effect is that the phase of the refractive index grating is shifted by $\pi/2$ from the interference pattern.[1−3] The laser beams are themselves diffracted by the grating, resulting in a change in the intensities of the transmitted beams; the intensity of one beam appears to increase while that of the other appears to decrease. This phenomenon is known as asymmetric energy exchange in photorefractive two-beam coupling. The photorefractivity of a material is often evaluated on the basis of its two-beam coupling efficiency (diffraction efficiency).[3] One class of materials that exhibit high diffraction efficiency are glassy photoconductive polymer materials doped with high concentrations of NLO compounds. These materials have been studied extensively[4−13] and have been shown to exhibit high diffraction efficiency (η) under the application of a ∼80 V/μm electric field. The photorefractivity of organic materials is greater than that of inorganic materials due to the higher Pockels constant and the ability of component chromophores to reorientate in the internal electric field. The photorefractive effect primarily induced by chromophoric reorientation is known as the orientational photorefractive effect. Recently, the photorefractive effect of low-molecular-weight nematic liquid crystals has been investigated,[14−19] and the photoinduced changes in refractive index in such crystals has been shown to be caused by changes in the orientation of liquid crystal molecules induced by the photoinduced space-charge field. The effect of the reorientation of liquid crystal molecules on the apparent refractive index is particularly strong. Despite these advantages of organic photorefractive materials, their response time is too slow (usually ∼100 ms) for practical applications, attributable to the slow reorientation of chromophores. The use of high-T_g polymers has been investigated as one means of addressing this problem.[20,21] In such stiff materials, the reorientation of chromophores is restricted, and refractive index modulation occurs solely due to the electrooptic effect. Although rapid response times have been achieved in these materials, the reported diffraction efficiencies are lower than in low-T_g materials due to the absence of a supplementary orientational mechanism.

In this study, we carried out a two-beam coupling experiment on surface-stabilized ferroelectric liquid crystals (SS-FLCs) doped with photoconductive compounds. Recently, the present authors[22,23] and Wasielewski et al.[24] independently reported the first observation of asymmetric energy exchange in FLCs; however, the photorefractivity of FLCs has yet to be characterized in detail. FLCs exhibit spontaneous polarization and are known to be sensitive to electric fields,[25] and the direction of spontaneous polarization is expected to be governed by the internal space-charge field. The refractive index grating is then considered to be created through the orientation of FLC molecules according to the direction of polarization. We prepared a series of FLC samples with different properties, and examined the effects of temperature, applied electric field, and magnitude of spontaneous polarization on the photorefractive properties of these SS-FLCs.

Experimental Section

Samples. The ferroelectric liquid crystals used in this study are commercially available from Chisso Chemical Corporation (Japan). The properties of these FLCs are listed in Table 1. The structures of the photoconductive compounds and the electron trap reagent are shown in Figure 1. The photoconductive compound, CDH, was synthesized via the reaction of diphenylhydrazine and *N*-ethylcarbazole-3-carboxaldehyde in pyridine. A photoconductive polymer PDPH was also synthesized. To increase the miscibility of the polymer with FLCs, a flexible spacer was incorporated between the chromophore and the polymer main chain. The number-average molecular weight of

* Author to whom correspondence should be addressed.

10.1021/jp0134493 CCC: $22.00 © 2002 American Chemical Society
Published on Web 02/14/2002

TABLE 1: Physical Properties of FLCs Used in This Study

	Ps at 25 °C (nC/cm^2)	phase transition temperature[a] (°C)	response time τ^b (μs)	tilt angle (deg.)
CS1011 (in 2 μm-gap cell)	13.0	− Sc* 56 S_A 77 N* 91 I	899	22
CDH 2 wt % (in 10 μm-gap cell)	2.2	− Sc* 47 S_A 71 N* 88 I		
CS1015 (in 2 μm-gap cell)	6.6	C −17 Sc* 58 S_A 68 N* 78 I	188	26
CDH 2 wt % (in 10 μm-gap cell)	3.2	Sc* 46 S_A 61 N* 76 I		
CS1022 (in 2 μm-gap cell)	34.7	C −11 Sc* 61 S_A 73 N* 85 I	56	25
CDH 2 wt % (in 10 μm-gap cell)	25.0	Sc* 54 S_A 68 N* 83 I		
CS1030 (in 2 μm-gap cell)	20.2	C −5 Sc* 70 S_A 74 N* 88 I	82	28
CDH 2 wt % (in 10 μm-gap cell)	14.4	Sc* 53 S_A 72 N* 86 I		

[a] C, crystal; Sc*, chiral smectic C phase; S_A, smectic A phase; N* chiral nematic phase; I, isotropic phase. [b] Response time to 10 V/μm electric field at 25 °C in a 2-μm cell.

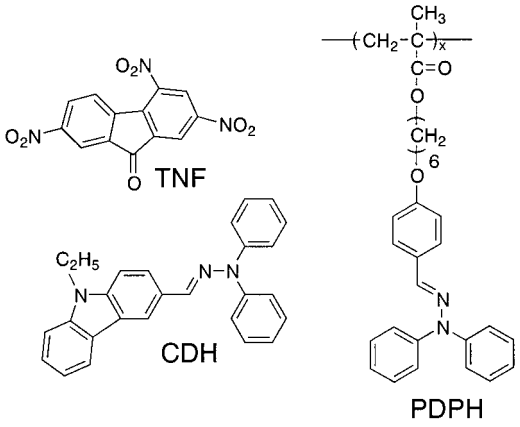

Figure 1. Structures of photoconductive compounds (CDH and PDPH) and electron trap reagent TNF.

PDPH was 12000 (M_w/M_n = 1.21), as measured by gel permeation chromatography (GPC). TNF (sensitizer/electron trap reagent) was obtained from Tokyo Kasei Co. (Japan) and purified by recrystallization from a hexanes−ethyl acetate mixture. The concentration of CDH was 2 wt %, and that of TNF was 0.1 wt %. The FLCs and dopants were dissolved in dichloroethane and the solvent was evaporated. The mixture was then dried in a vacuum at room temperature for one week. At this concentration, no phase separation was observed under a polarizing microscope or in differential scanning calorimeter (DSC) measurements. Phase separation was observed at CDH concentrations exceeding 3 wt %. The samples were injected into a 10 μm-gap glass cell equipped with 1 cm^2 ITO electrodes and a polyimide alignment layer. A 2 to 5 μm-gap cell is typically used to obtain a surface-stabilized FLC;[25] however, finely aligned FLC samples were obtained using the 10 μm-gap cell.

Measurement. The phase transition temperatures were determined by DSC (SSC-5000, Seiko I&E, Japan) and by microscope (FP-80 and FP-82, Mettler, BX-50 polarizing microscope, Olympus). The photoconductivity was measured using a R8340 ultrahigh-resistance ohmmeter (Advantest Inc., Japan). The photorefractive effect was measured in a two-beam coupling experiment. A schematic illustration of the experimental setup is shown in Figure 2. A p-polarized beam from an Ar^+ laser (165LGS−S, Laser Graphics; 488 nm, continuous wave) was divided by a beam splitter and refocused in the sample film. The intensity of the laser was 2.4 mW for each beam (1-mm diameter). The sample was inclined at 50°, and the angle between the two incident beams was set to 20°, producing a grating spacing (Λ) of 1.9 μm inside the material (n = 1.65). The sample was thermostated using a thermocontroller (DB1000, Chino Co). An electric field of 0∼10 V/μm was applied to the sample using a regulated DC power supply (DW36-1, Kenwood), and the change in transmitted beam intensity was monitored by a power meter (TQ8210+TQ82014, Advantest Inc.) and recorded by computer. The spontaneous polarization of FLCs was measured by the triangular voltage method (10 Vp-p, 100 Hz).

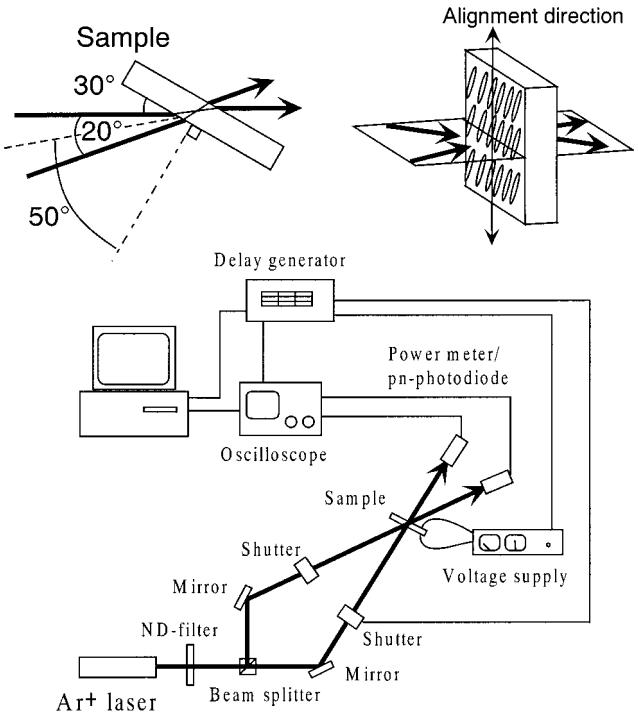

Figure 2. Schematic of experimental setup for two-beam coupling.

Results and Discussion

Two-Beam Coupling Experiment on FLCs. Figure 3 shows a typical example of the asymmetric energy exchange observed in the CDH/TNF/CS1011 sample. An electric field of 0.1 V/μm

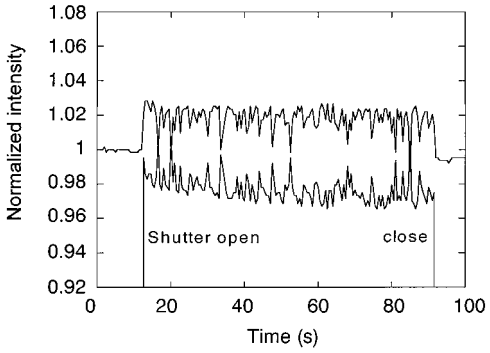

Figure 3. Typical example of asymmetric energy exchange observed in CS1011 mixed with 2 wt % CDH and 0.1 wt % TNF.

was applied to the sample. The interference of the divided beams in the sample resulted in the increased transmittance of one of the beams and the reduced transmittance of the other beam. These transmittance characteristics were reversed when the polarity of the applied electric field was reversed. The diffraction efficiency is defined as $\Delta I/I_0$, where I_0 is the transmitted beam intensity without interference (one of the beams blocked), and ΔI is the change in transmittance caused by the beam coupling. A diffraction efficiency of 2.48% was obtained at 27 °C. Asymmetric energy exchange was observed only when an electric field was applied, indicating that beam coupling was not caused by a thermal grating. To calculate the two-beam coupling gain coefficient, the diffraction condition needs to be correctly identified. The two possible diffraction conditions are the Bragg regime and the Raman-Nath regime, distinguished by the dimensionless parameter Q.[2]

$$Q = 2\pi\lambda L/n\Lambda^2 \tag{1}$$

where L is the interaction wavelength; here, $L = 13$ μm. $Q > 1$ is defined as the Bragg regime of optical diffraction. In this regime, multiple scattering is not permitted and only one order of diffraction of light is produced. Conversely, $Q < 1$ is defined as the Raman-Nath regime of optical diffraction, in which many orders of diffraction can be observed. $Q > 10$ is usually required to guarantee that diffraction occurs entirely in the Bragg regime. Under the present experimental conditions, Q is calculated to be 6.6. Therefore, the diffraction observed in this experiment occurs predominantly, but not entirely, in the Bragg regime, with a small Raman-Nath component. However, since higher-order diffraction was not observed, we calculated the two-beam coupling gain coefficient Γ according to the equation assuming Bragg diffraction, as follows:[1,2,9]

$$\Gamma = \frac{1}{D}\ln\left(\frac{gm}{1+m-g}\right) \tag{2}$$

where $D = l/\cos(\theta)$ is the interaction path for the signal beam (l = sample thickness, θ = propagation angle of the signal beam in the sample), g is the ratio of intensities of the signal beam behind the sample with and without a pump beam, and m is the ratio of the beam intensities (pump/signal) in front of the sample. The gain coefficient at 30 °C was calculated to be 31.3 cm^{-1} for a CDH/TNF/CS1011 sample. The total optical loss (including absorption, scattering, reflection, etc.) was found to be 30 cm^{-1}, primarily attributable to reflection.

Effect of Temperature. The temperature dependence of the diffraction efficiency of CS1011 doped with 2 wt % CDH and 0.1 wt % TNF is shown in Figure 4. Asymmetric energy exchange was observed only at temperatures below 45 °C. The

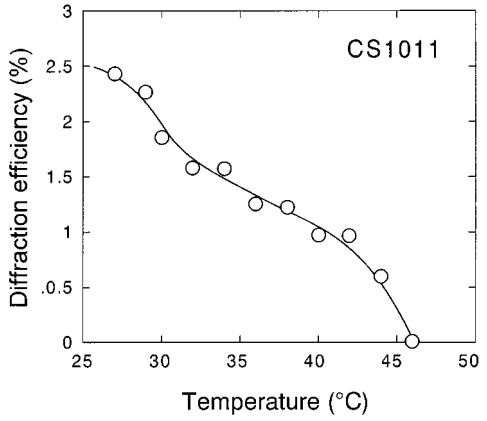

Figure 4. Temperature dependence of diffraction efficiency of CS1011 mixed with 2 wt % CDH and 0.1 wt % TNF. An electric field of 0.1 V/μm was applied to the sample.

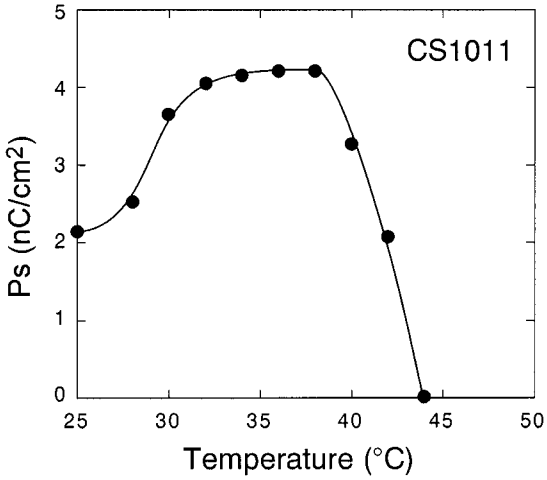

Figure 5. Temperature dependence of spontaneous polarization of CS1011 mixed with 2 wt % CDH and 0.1 wt % TNF measured by triangular voltage method (100 Hz, 10 Vp-p) in a 10 μm-gap-cell.

spontaneous polarization of the CS1011/CDH/TNF mixture in the 10 μm-gap cell is plotted as a function of temperature in Figure 5. The spontaneous polarization vanished when the temperature was raised above 45 °C. Thus, asymmetric energy exchange was observed only in the temperature range in which the sample exhibits ferroelectric properties (Sc* phase). The two-beam coupling experiment was also performed on the FLCs listed in Table 1. The temperature dependence of the diffraction efficiencies of these FLCs and the spontaneous polarization are shown in Figures 6−8. The results are similar to those for CS1011. Asymmetric energy exchange was observed only in the Sc* phase. Many of the nematic liquid crystalline photorefractive materials reported to date, usually cyanobiphenyl liquid crystals, possess a large dipole moment aligned in the same direction as the molecular axis. In these nematic liquid crystals, a refractive index grating is generated as a result of orientational fluctuation along the director axis caused by the photoinduced internal electric field. In contrast, the molecular dipole moment of FLCs is small and the dipole moment is aligned perpendicular to the molecular axis. Large changes in the orientation of the molecular axis could be induced by the internal electric field in the S_A or N* phase of the FLCs used in this study. However, in the Sc* phase, reorientation associated with spontaneous polarization occurred due to the internal electric field. Spontaneous polarization causes the orientation of mesogens in the corresponding area to change accordingly.

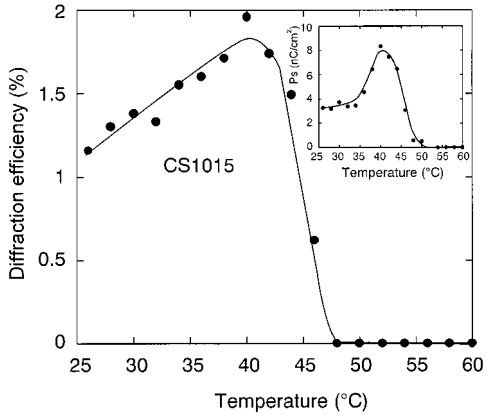

Figure 6. Temperature dependence of diffraction efficiency of CS1015 mixed with 2 wt % CDH and 0.1 wt % TNF. An electric field of 0.1 V/μm was applied to the sample. Inset shows temperature dependence of spontaneous polarization of the mixture in a 10 μm-gap-cell.

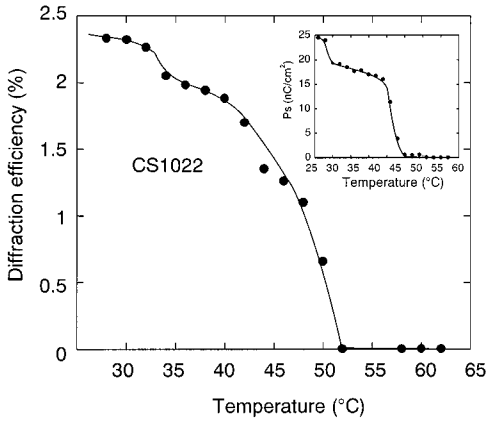

Figure 7. Temperature dependence of diffraction efficiency of CS1022 mixed with 2 wt % CDH and 0.1 wt % TNF. An electric field of 0.1 V/μm was applied to the sample. Inset shows temperature dependence of spontaneous polarization of the mixture in a 10 μm-gap-cell.

Effect of Magnitude of Applied Electric Field. The photorefractive effect in FLCs can be induced by the application of very weak external electric fields. In polymer materials, an electric field of 10−50 V/μm is necessary to induce photorefractivity, whereas the maximum diffraction efficiency of the CS1011 sample was obtained using an electric field strength of only 0.1−0.2 V/μm. The dependence of the diffraction efficiency of CDH/TNF/FLCs on the strength of the electric field is shown in Figure 9. The dependence is quite different from that of nematic liquid crystals and amorphous polymers. In nematic liquid crystals (and amorphous polymers), the diffraction efficiency exhibits a $\sin^2$ dependence on the electric field, which can be correlated with Kogelnik's theory.[26] However, in FLC, the dependence of the diffraction efficiency on the strength of the external electric field is different from the dependence observed for the range of nematic LCs reported to date.[14−19] The diffraction efficiency of CDH/TNF/CS1011 increases with the strength of the external electric field up to 0.2 V/μm, above which the diffraction efficiency decreases. As shown in Figure 9, the same tendency was observed in CS1015, CS1022, and CS1030. The formation of the orientational grating is enhanced when the external electric field is increased from 0 to 0.2 V/μm, as a result of the charge separation induced under a higher external electric field. However, when the external electric field exceeded 0.2 V/μm, the dipole moments of mesogens were constrained to the direction of the external electric field.

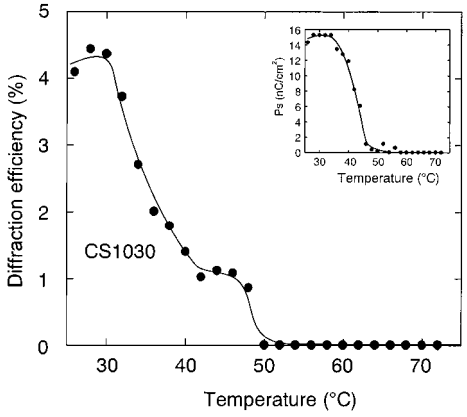

Figure 8. Temperature dependence of diffraction efficiency of CS1030 mixed with 2 wt % CDH and 0.1 wt % TNF. An electric field of 0.1 V/μm was applied to the sample. Inset shows temperature dependence of spontaneous polarization of the mixture in a 10 μm-gap-cell.

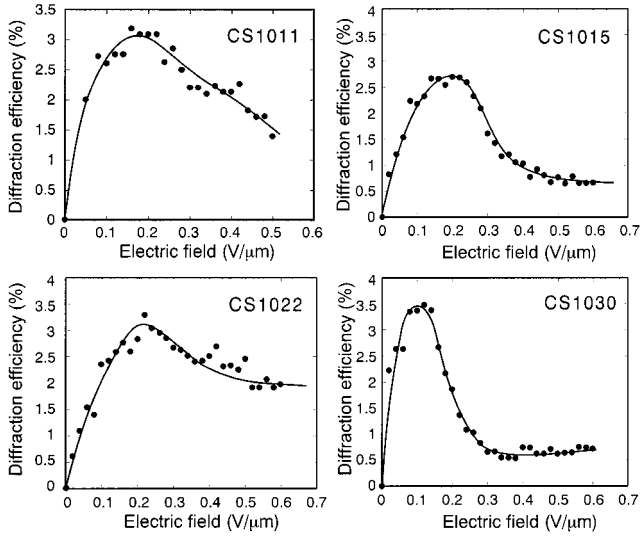

Figure 9. Electric field dependence of diffraction efficiency of FLCs mixed with 2 wt % CDH and 0.1 wt % TNF in a 10 μm-gap-cell measured at 30 °C.

Refractive Index Grating Formation Time. The refractive index grating formation time in CDH/TNF/CS1011 was measured on the basis of the simplest single-carrier model of photorefractivity,[2] in which the gain transient is exponential. The rising signal of the diffracted beam was fitted by a single-exponential function:

$$\gamma(t) - 1 = (\gamma - 1)[1 - \exp(-t/\tau)] \qquad (3)$$

where $\gamma(t)$ represents the transmitted beam intensity at time t divided by the initial intensity ($\gamma(t) = I(t)/I_0$) and τ is the formation time. The grating formation time in CDH/TNF/CS1011 is plotted as a function of the strength of the external electric field in Figure 10. The grating formation time decreases with increasing electric field strength, presumably due to the increased efficiency of charge generation. The formation time was shorter at higher temperatures. The viscosity of FLC decreases with rising temperature, such that the formation time decreases at higher temperatures. The formation time was found to be 28.8 ms at 36 °C.

Photorefractive Effect in Photoconductive Polymer/FLC Mixture. The photorefractivity of the mixture of FLC and photoconductive polymer (PDPH) was also measured. As shown in Figure 11, the PDPH film doped with 1 wt % TNF clearly

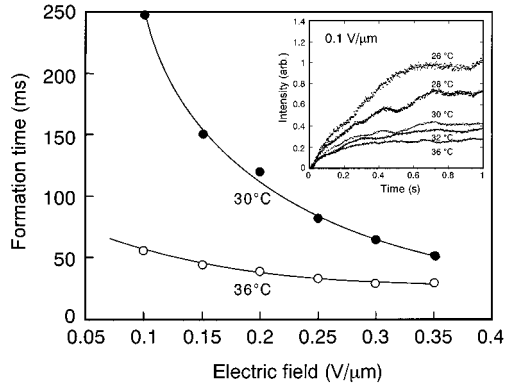

Figure 10. Electric field dependence of index grating formation time of CS1011 mixed with 2 wt % CDH and 0.1 wt % TNF in two-beam coupling experiment. ●, measured at 30 °C; ○, measured at 36 °C. Inset shows rising signals under application of 0.1 V/μm external electric field.

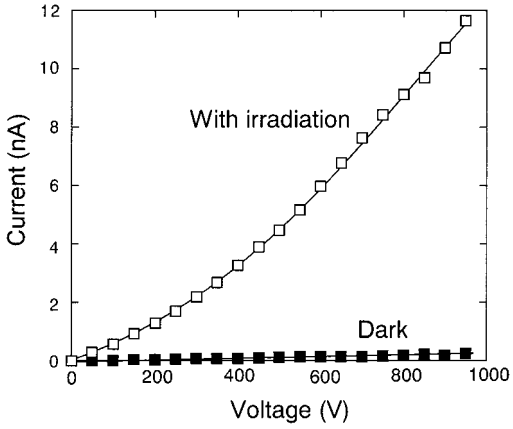

Figure 11. Electric field dependence of photocurrent of PDPH film (100-μm thick) doped with 1 wt % TNF. A beam from an Ar^+ laser (488 nm, CW) was used as the light source. Intensity of 1 mm-diameter beam: 10 mW. □, irradiated; ■, in darkness.

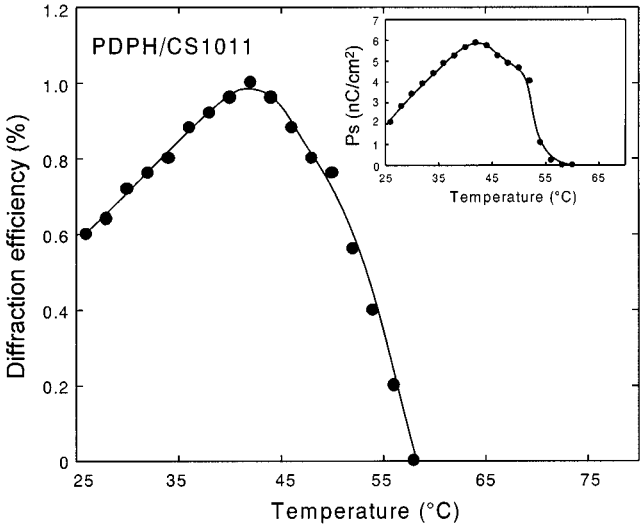

Figure 12. Temperature dependence of diffraction efficiency of CS1011 mixed with 2 wt % PDPH and 0.1 wt % TNF. An electric field of 0.1 V/μm was applied to the sample. Inset shows temperature dependence of spontaneous polarization of the mixture in a 10 μm-gap-cell.

exhibited photoconductivity. The diffraction efficiency of CS1011 mixed with 2 wt % PDPH and 0.1 wt % TNF was then investigated. The alignment of the FLC was disturbed to some extent by the incorporation of PDPH; however, no phase separation was observed at a concentration of 2 wt %. The temperature dependence of the diffraction efficiency of the PDPH/CS1011 mixture is shown in Figure 12. The diffraction efficiency increased with temperature up to 42 °C, then decreased and vanished by 58 °C, corresponding directly to the temperature dependence of spontaneous polarization (Figure 12 inset). Although the memory effect of nematic LC/polymer mixtures, representing the index grating remaining after writing beams are removed, has been reported previously,[27] the memory effect was not observed in PDPH/FLC mixtures. The dependence of the diffraction efficiency of PDPH/CS1011 on electric field strength is shown in Figure 13. The diffraction efficiency of this material also increases with electric field strength up to 0.2 V/μm; however the subsequent decrease observed for CDH/TNF/FLCs is not as prominent in this case.

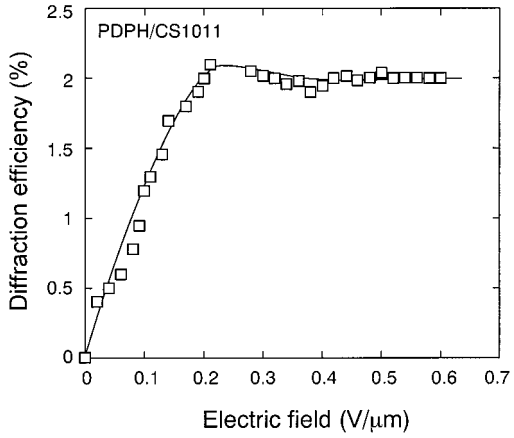

Figure 13. Electric field dependence of diffraction efficiency of CS1011 mixed with 2 wt % PDPH and 0.1 wt % TNF measured at 30 °C.

Conclusion

The photorefractivity of a series of FLC mixtures was investigated through two-beam coupling experiments. The reorientational photorefractive effect was observed in dye-doped FLC samples. Photorefractivity was observed only in the ferroelectric phase of these samples, and the refractive index formation time was found to be shorter than that of nematic LCs. These results indicate that the mechanism responsible for refractive index grating formation in FLCs is different from that for nonferroelectric materials, and is clearly related to the ferroelectric properties of the material.

Acknowledgment. We are grateful for financial support from the Murata Science Foundation.

References and Notes

(1) Solymar, L.; Webb, J. D.; Grunnet-Jepsen, A. *The Physics and Applications of Photorefractive Materials*; Oxford: New York, 1996.

(2) Yeh, P. *Introduction to Photorefractive Nonlinear Optics*; John Wiley: New York, 1993.

(3) Moerner, W. E.; Silence, S. M. *Chem. Rev.* **1994**, *94*, 127.

(4) Meerholz, K.; Volodin, B. L.; Kippelen, B.; Peyghambarian, N. *Nature* **1994**, *371*, 497.

(5) Volodin, B. L.; Kippelen, B.; Meerholz, K.; Javidi, B.; Peyghambarian, N. *Nature* **1996**, *383*, 58.

(6) Chan, W.-K.; Chen, Y.; Peng, Z.; Yu, L. *J. Am. Chem. Soc.* **1993**, *115*, 11735.

(7) Peng, Z.; Bao, Z.; Yu, L. *J. Am. Chem. Soc.* **1994**, *116*, 6003.

(8) Peng, Z.; Gharavi, A. R.; Yu, L. *J. Am. Chem. Soc.* **1997**, *119*, 4622.

(9) Cui, Y.; Swedek, B.; Cheng, N.; Kim, K.-S.; Prasad, P. N. *J. Phys. Chem. B* **1997**, *101*, 3530.

(10) Grunnet-Jepsen, A.; Thompson, C. L.; Moerner, W. E. *Science* **1997**, *277*, 549.
(11) Kippelen, B.; Marder, S. R.; Hendrickx, E.; Maldonado, J. L.; Guillemet, G.; Volodin, B. L.; Steele, D. D.; Enami, Y.; Sandalphon; Yao, Y. J.; Wang, J. F.; Röckel, H.; Erskine, L.; Peyghambarian, N. *Science* **1998**, *279*, 54.
(12) Meerholz, K.; Nardin, Y. D.; Bittner, R.; Wortmann, R.; Würthner, F. *Appl. Phys. Lett.* **1998**, *73*, 4.
(13) Hendrickx, E.; Wang, J. F.; Maldonado, J. L.; Volodin, B. L.; Mash, E. A.; Persoons, A.; Kippelen, B.; Peyghambarian, N. *Macromolecules* **1998**, *31*, 734.
(14) Khoo, I. C.; Li, H.; Liang, Y. *Opt. Lett.* **1994**, *19*, 1723.
(15) Rudenko, E. V.; Sukhov, A. V. *JETP* **1994**, *78*, 875.
(16) Wiederrecht, G. P.; Yoon, B. A.; Wasielewski, M. R. *Science* **1995**, *270*, 1794.
(17) Wiederrecht, G. P.; Yoon, B. A.; Svec, W. A.; Wasielewski, M. R. *J. Am. Chem. Soc.* **1997**, *119*, 3358.
(18) Wiederrecht, G. P.; Waiselewski, M. R. *J. Am. Chem. Soc.* **1998**, *120*, 3231.
(19) Ono, H.; Kawatsuki, N. *Jpn. J. Appl. Phys.* **1997**, *36*, 6444.
(20) Hattemer, E.; Zentel, R.; Mecher, E.; Meerholz, K. *Macromolecules* **2000** *33*, 1972.
(21) Hofmann, U.; Grasruck, M.; Leopold, A.; Schreiber, A.; Schloter, S.; Hohle, C.; Strohriegel, P.; Haarer, D.; Zilker, S. J. *J. Phys. Chem. B* **2000**, *104*, 3887.
(22) Sasaki, T. *Polymer Applications (Koubunshi Kakou)* **2000**, *49*, 214.
(23) Sasaki, T.; Shibata, M.; Kino, Y.; Ishikawa, Y.; Yoshimi, T. *Polym. Prepr. Jpn.* **2000**, *49*, 704.
(24) Wiederrecht, G. P.; Yoon, B. A.; Wasielewski, M. R. *Adv. Mater.* **2000**, *12*, 1533.
(25) Skarp, K.; Handschy, M. A. *Mol. Cryst. Liq. Cryst.* **1988**, *165*, 439.
(26) Kogelnik, H. *Bell Syst. Technol. J.* **1969**, *48*, 2909.
(27) Ono, H.; Kawatsuki, N. *J. Appl. Phys.* **1999**, *85*, 2482.